

Some simple potentials

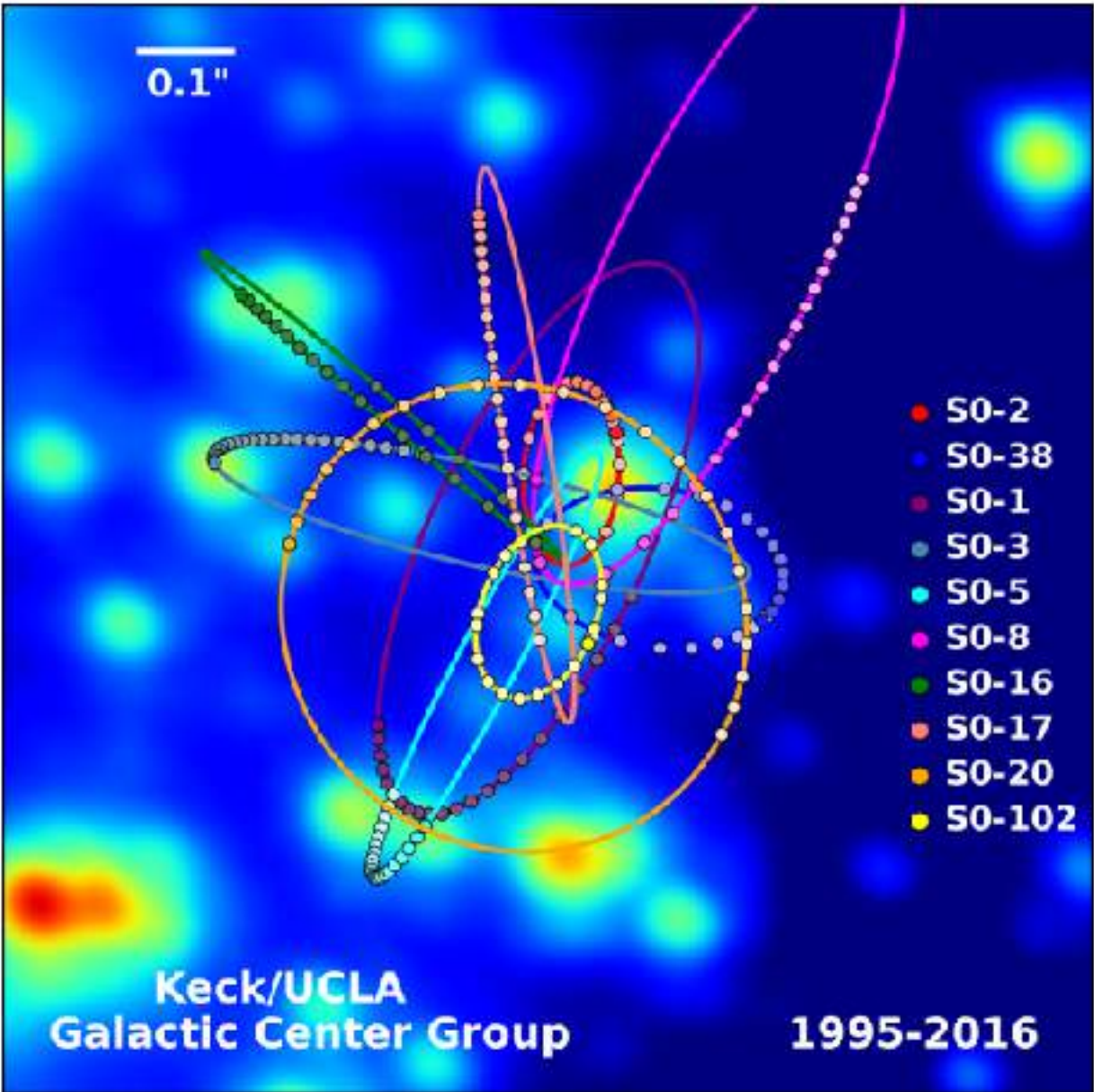
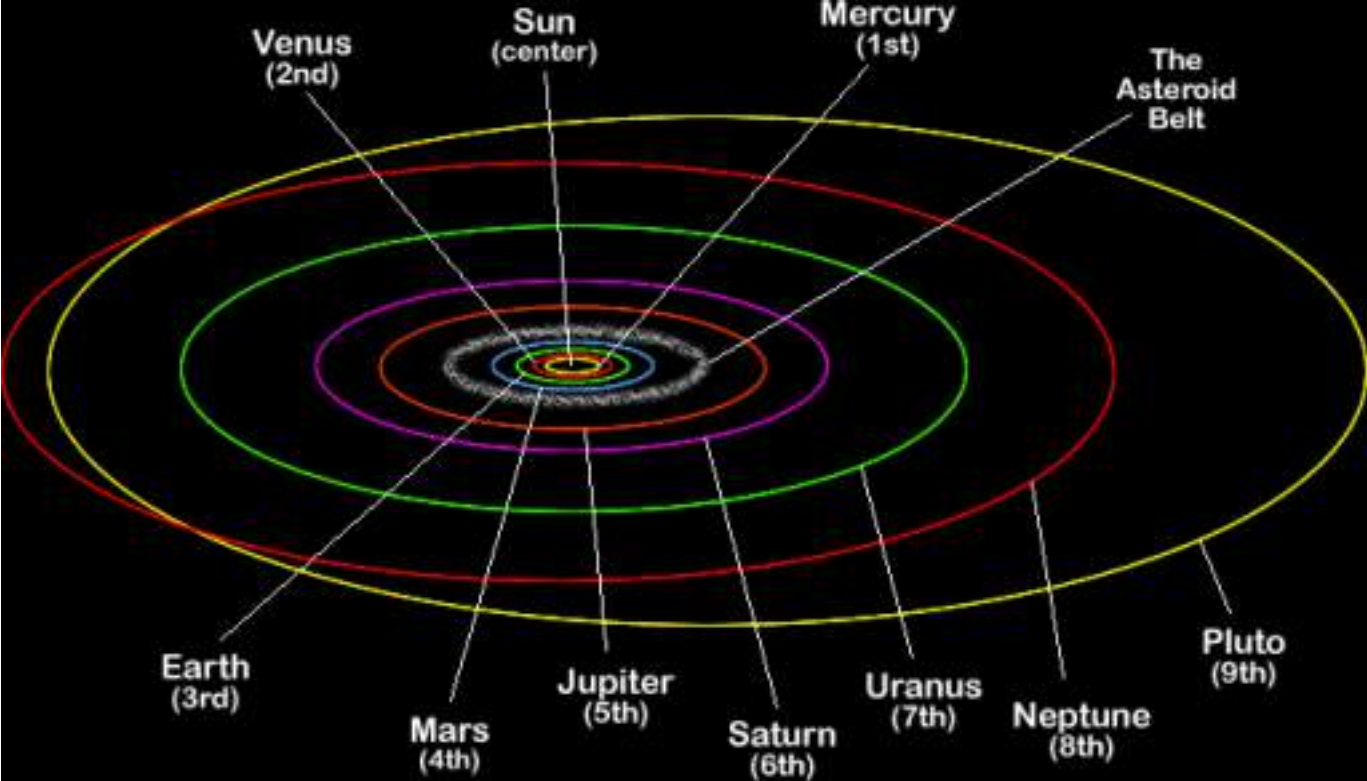
BT2, §2.2.2

Point mass (Keplerian)

$$\Phi(r) = -\frac{GM}{r}$$

$$v_c(r) = \left(\frac{GM}{r}\right)^{1/2}$$

$$v_e(r) = \left(\frac{2GM}{r}\right)^{1/2}$$



Planets around stars
Stars around massive black holes

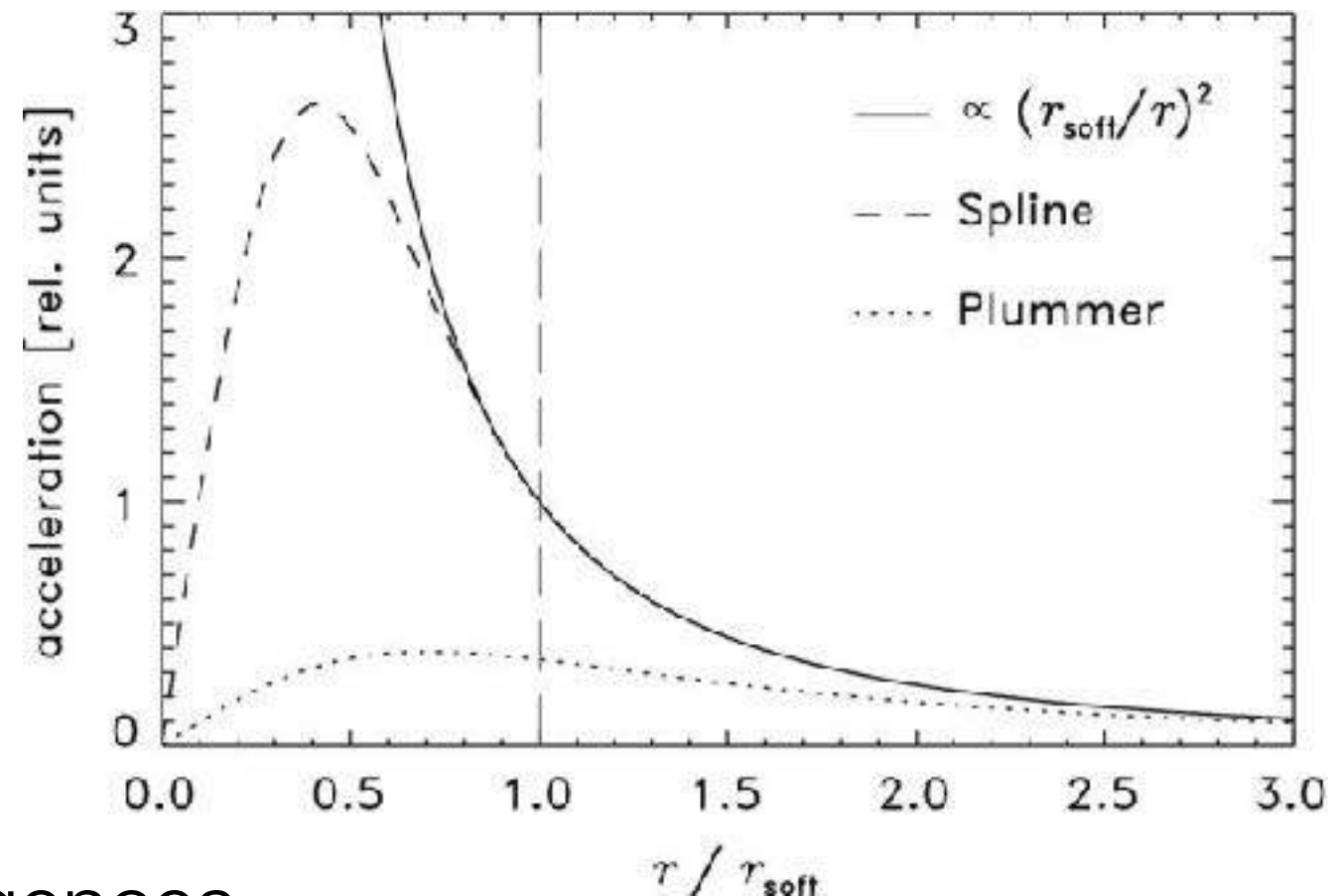
Plummer model

$$\Phi(r) = - \frac{GM}{\sqrt{r^2 + b^2}}$$

↑
Plummer scale length

$$\rho(r) = \frac{3M}{4\pi b^3} \left(1 + \frac{r^2}{b^2} \right)^{-5/2}$$

$\approx \text{const. inside } b$



Star clusters

Gravitational softening to avoid divergences

Homogeneous sphere

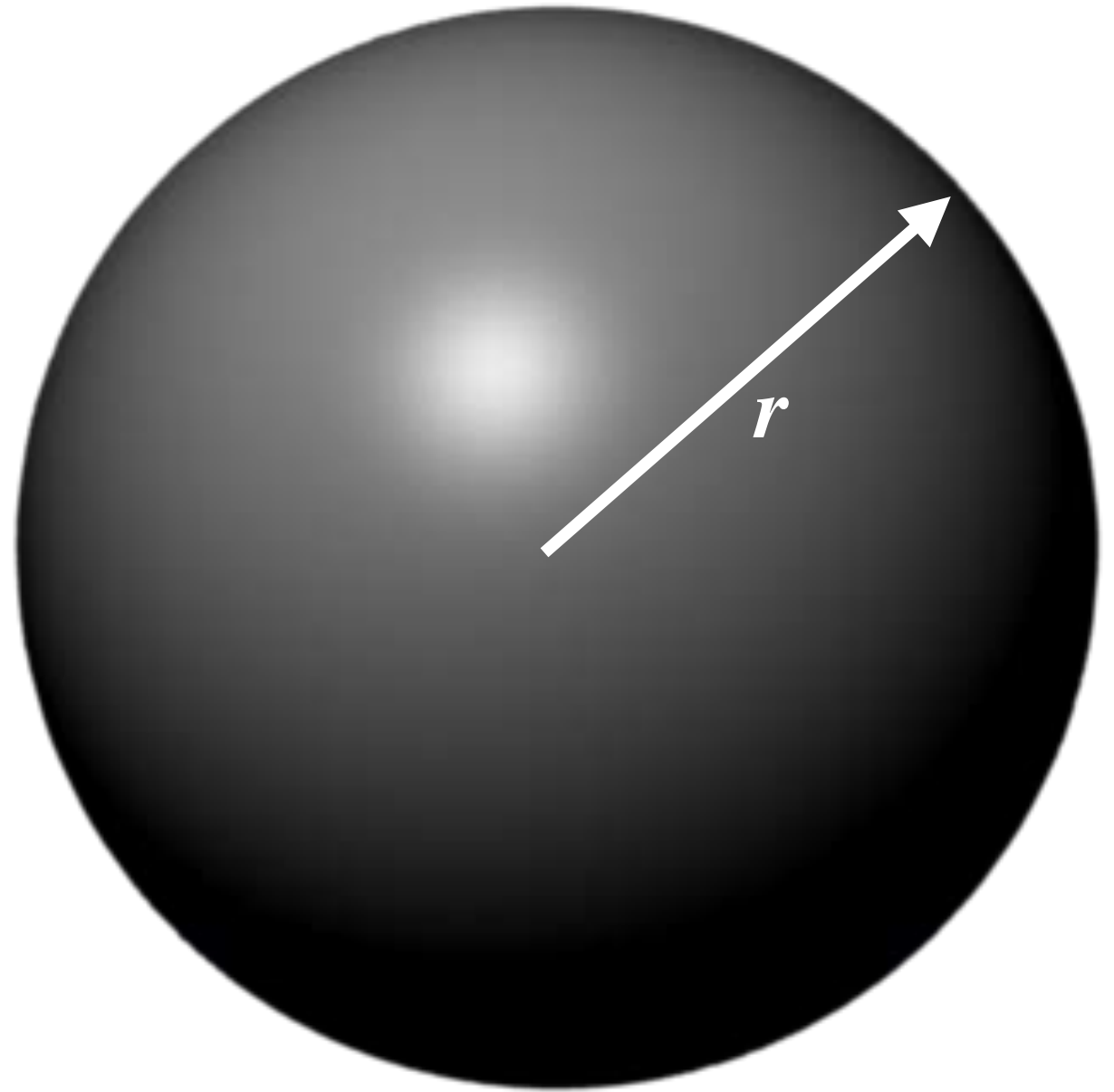
$$M(r) = \frac{4\pi r^3 \rho}{3}; \quad \rho = \text{const}$$

$$v_c(r) = \left(\frac{4\pi G \rho}{3} \right)^{1/2} r$$

Orbital period

$$T = \frac{2\pi r}{v_c} = \left(\frac{3\pi}{G\rho} \right)^{1/2}$$

independent of radius



Free fall/dynamical time

Radial acceleration

$$\frac{d^2 r}{dt^2} = -\frac{GM(r)}{r^2} = -\frac{4\pi G\rho}{3}r$$

Simple harmonic oscillator. Try solutions of the form $r = A \sin(\Omega t)$

Valid solution iff

$$\Omega = \left(\frac{4\pi G\rho}{3}\right)^{1/2}$$

Particle “dropped” at r reaches center in 1/4 period, i.e. free fall time

$$t_{\text{ff}} = \frac{T}{4} = \frac{1}{4} \frac{2\pi}{\Omega} = \left(\frac{3\pi}{16G\rho}\right)^{1/2} \approx \frac{0.767}{(G\rho)^{1/2}} \approx \frac{1}{(G\rho)^{1/2}}$$

Singular isothermal sphere

Special case of power-law model

$$\rho(r) = \rho_0 \left(\frac{r_0}{r} \right)^\alpha ; \alpha = 2$$

$$v_c = 4\pi G \rho_0 r_0^2 = \text{const.} \quad \text{hence, constant "temperature"}$$

Simple model for systems with flat rotation curve or vel. disp. profile

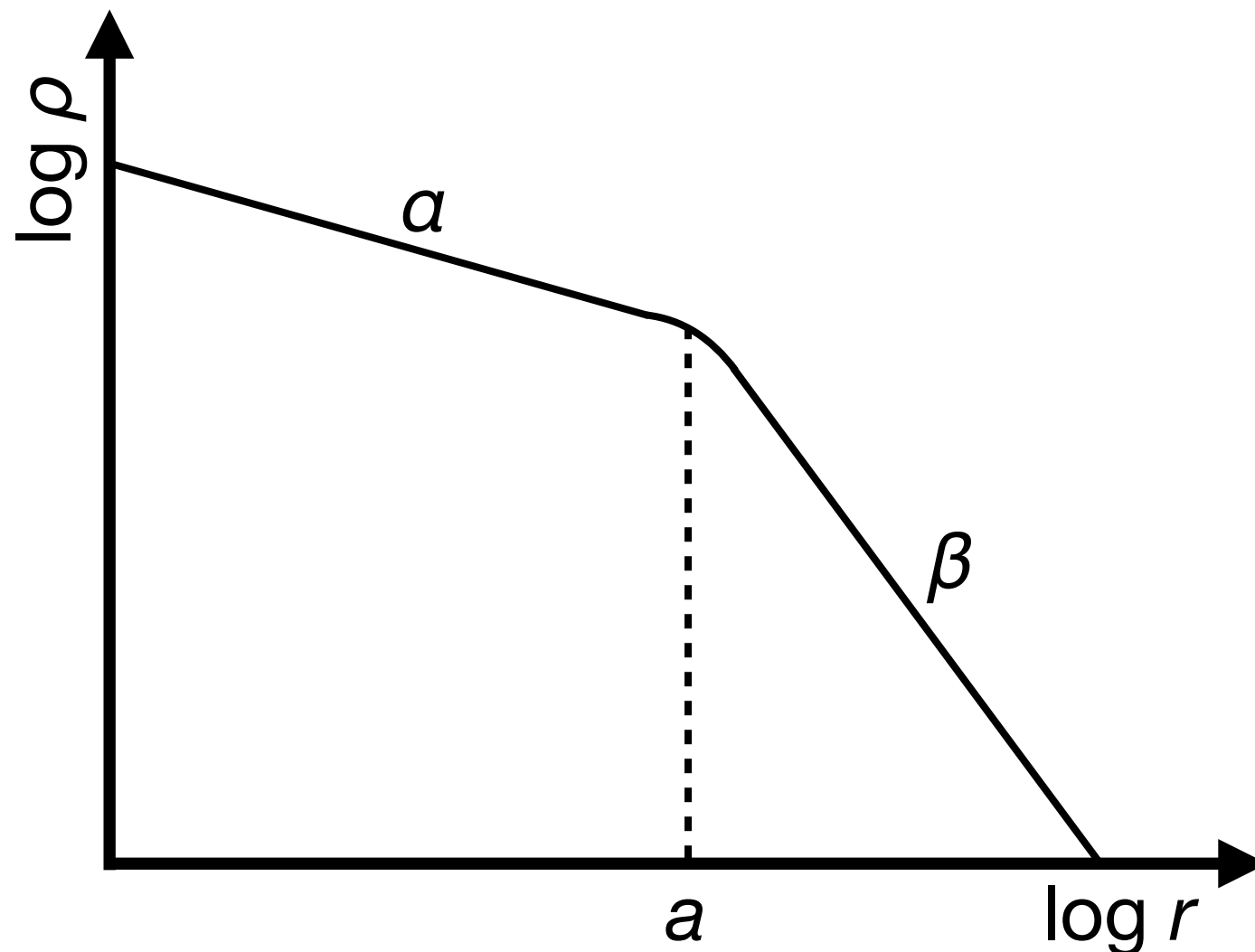
- fair approximation to many galaxies, some radii in dark matter halos
- often used for toy models
- usually unrealistic as $r \rightarrow 0$, since there $\rho \rightarrow \infty$

Two power-law density models

$$\rho(r) = \frac{\rho_0}{(r/a)^\alpha (1 + r/a)^{\beta-\alpha}}$$

Hernquist (1990) : $\alpha = 1, \beta = 4$ elliptical galaxies, galaxy bulges

NFW (1996) : $\alpha = 1, \beta = 3$ dark matter halos



de Vaucouleurs' $R^{1/4}$ law for ellipticals and bulges

A good fit to the light profile of many ellipticals and bulges:

$$\ln I(R) = \ln I_e + 7.669 \left[1 - \left(\frac{R}{R_e} \right)^{1/4} \right]$$

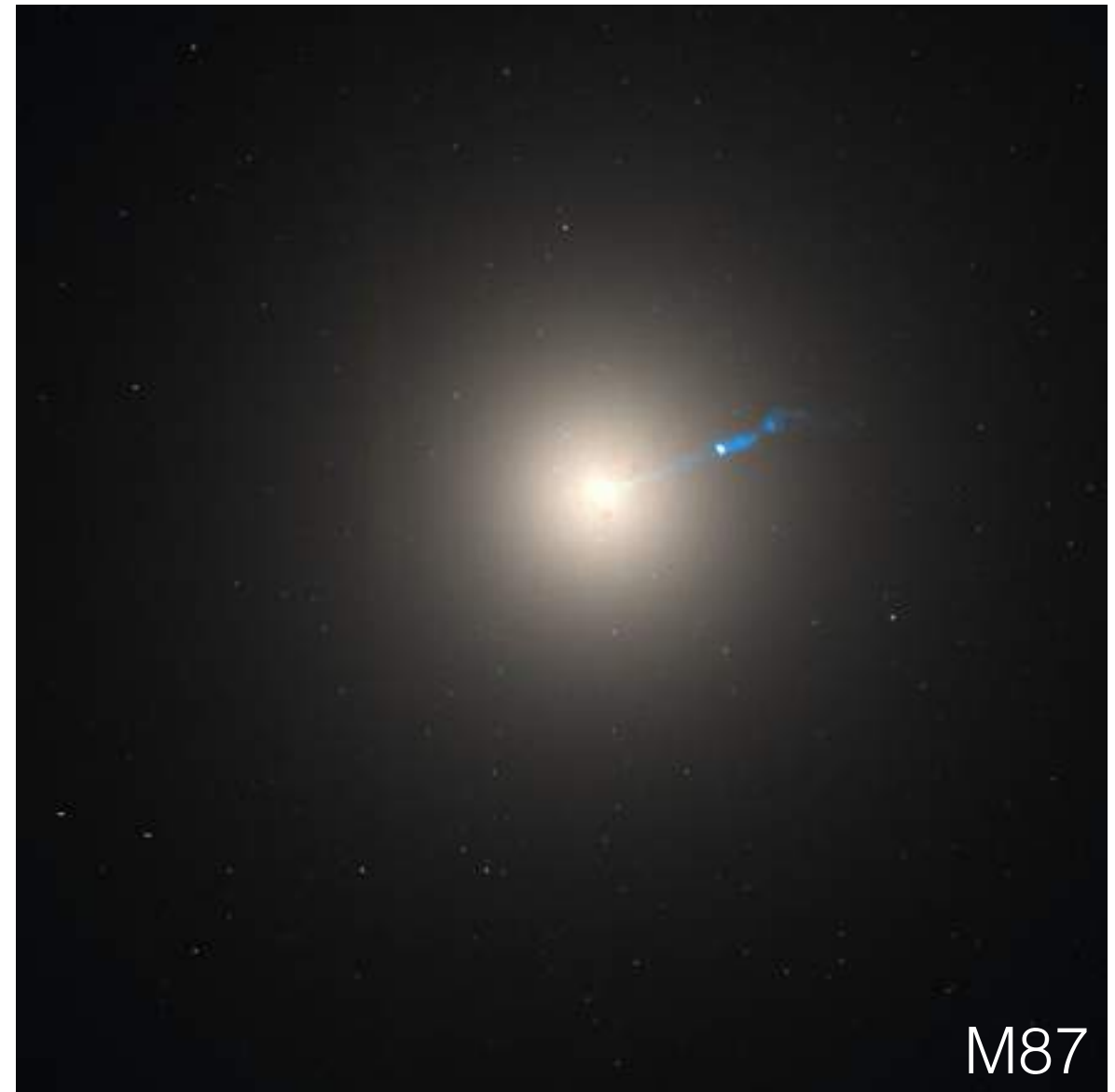
↑
(constant such that R_e
encloses 1/2 light)

I = surface brightness

R = projected radius

R_e = effective radius enclosing 1/2 of light

$$\int_0^{R_e} I(R) r dr = \frac{1}{2} \int_0^{\infty} I(R) r dr.$$



Sérsic profile

Generalization of de
Vaucouleurs' $R^{1/4}$ law

$$\ln I(R) = \ln I_0 - kR^{1/n}$$

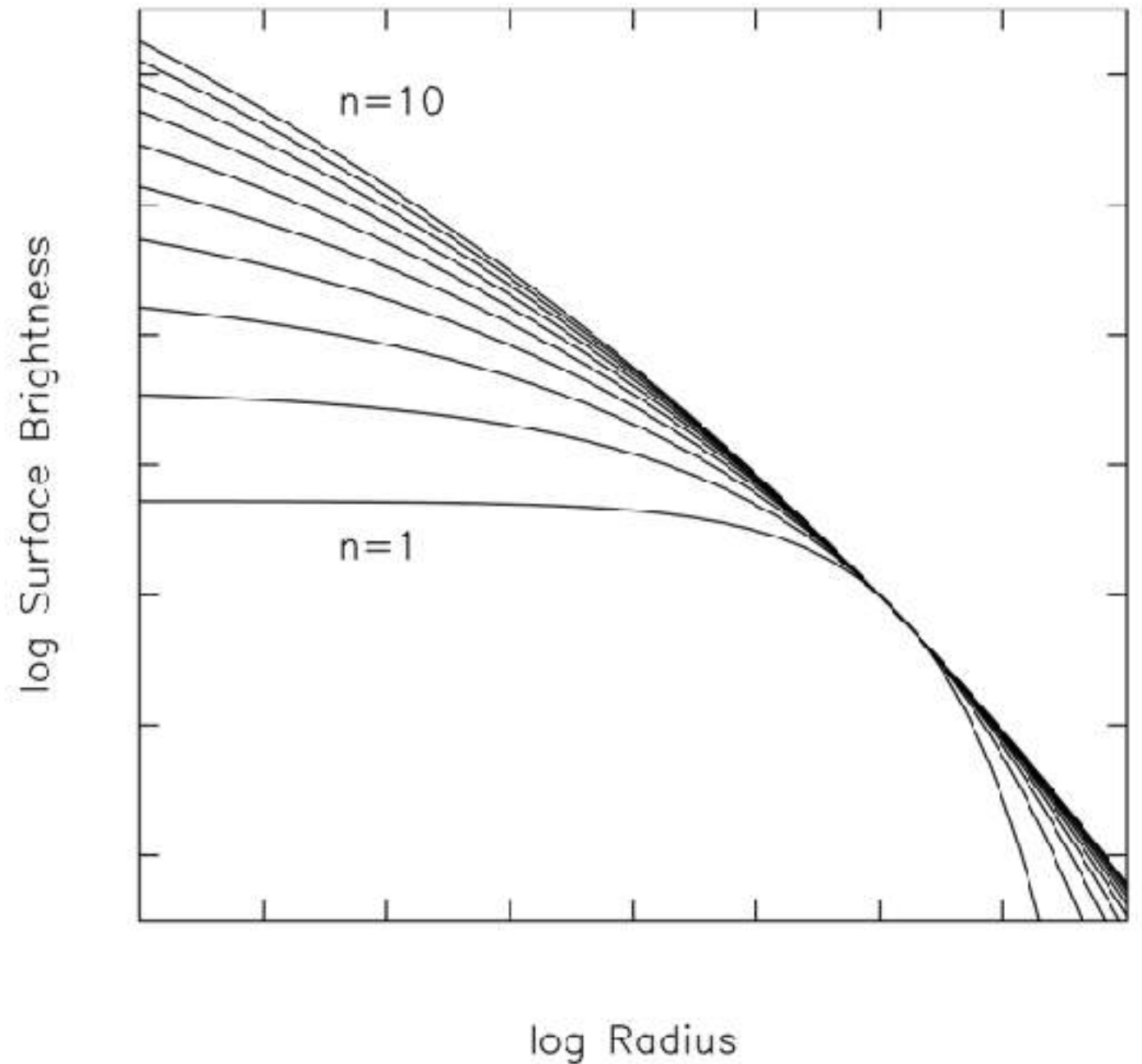
n =Sérsic index (=4 for $R^{1/4}$)

More luminous galaxies tend to
have larger n

$n=1$ gives exponential profile

$$I(R) \propto e^{-kR}$$

which is a good approximation to
many spirals



Hernquist profile

Sky projection is close to $R^{1/4}$ law, but 3D mass distribution is analytically tractable (unlike $R^{1/4}$):

$$\rho(r) = \frac{M a}{2\pi r} \frac{1}{(r + a)^3}$$

M = total mass

a = scale radius

Convenient for theoretical models of ellipticals and bulges

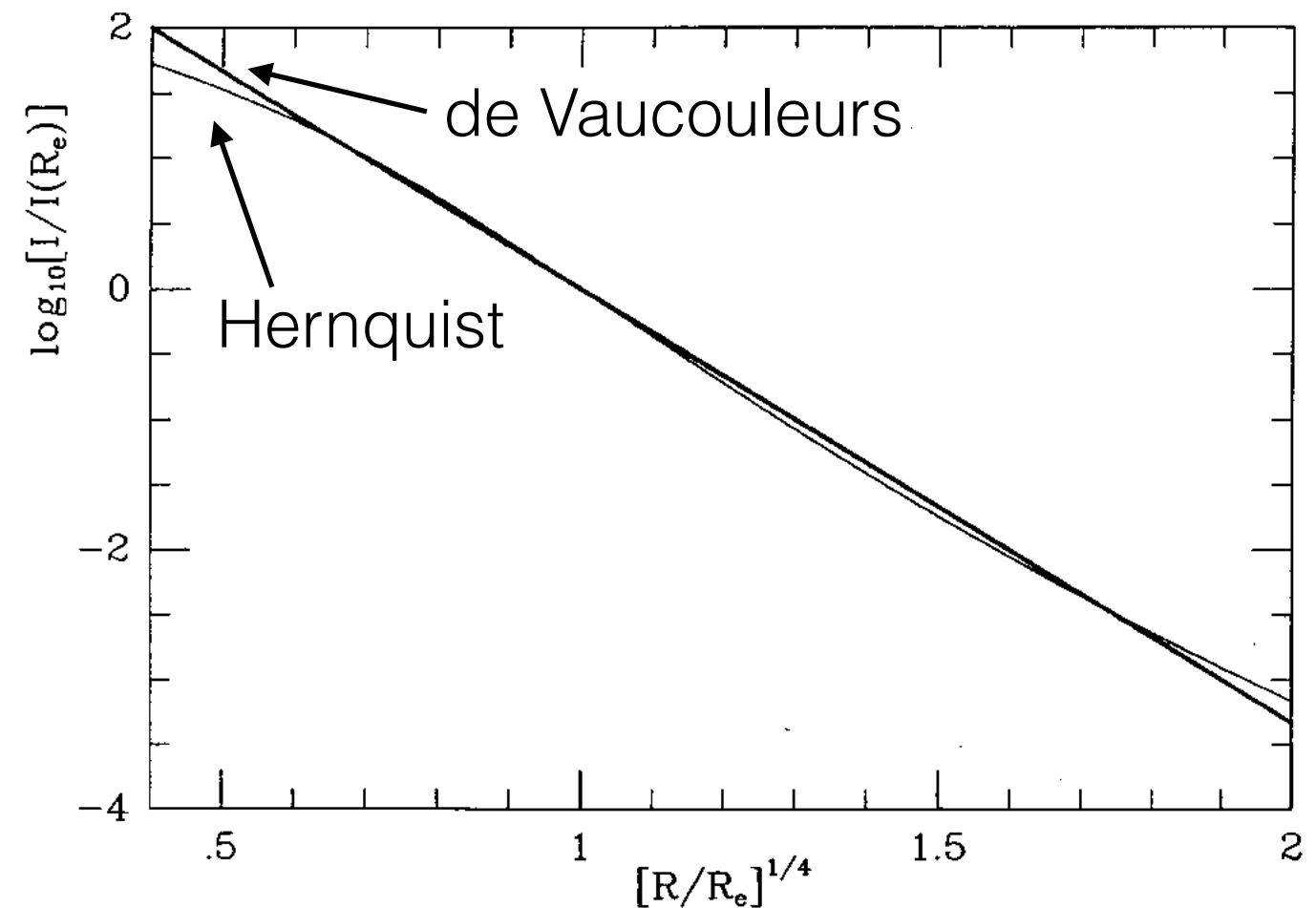
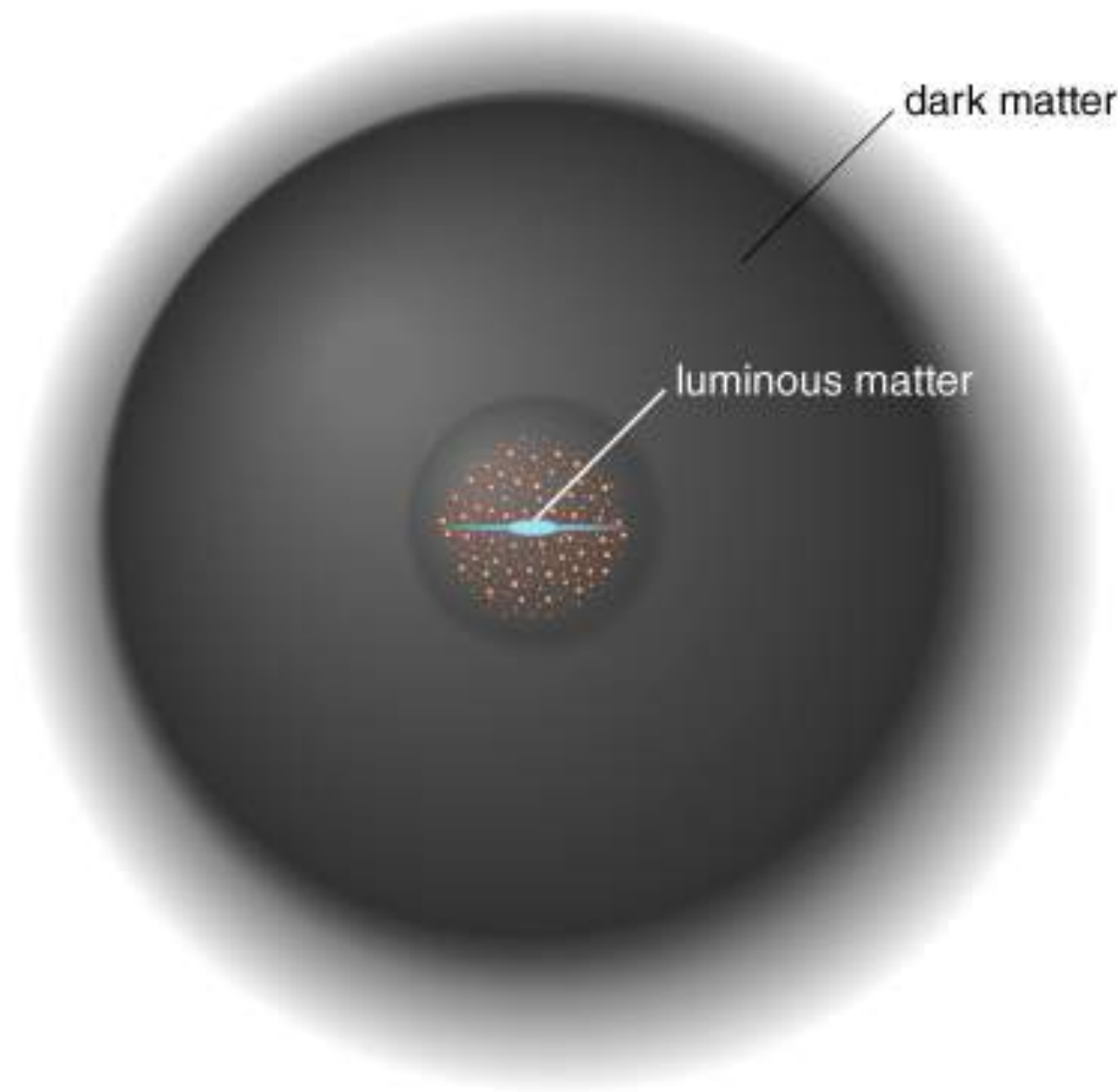


FIG. 4.—Surface brightness profiles for the $R^{1/4}$ law (*thick curve*) and the present model (*thin curve*) as a function of $(R/R_e)^{1/4}$. Surface brightness is normalized to its value at R_e where R_e refers separately to the effective radii of the two models.

**Dark matter halo properties
from
cosmological *N*-body simulations**

Dark halos are much larger than galaxies



E.g., Milky Way:

- scale length of stellar

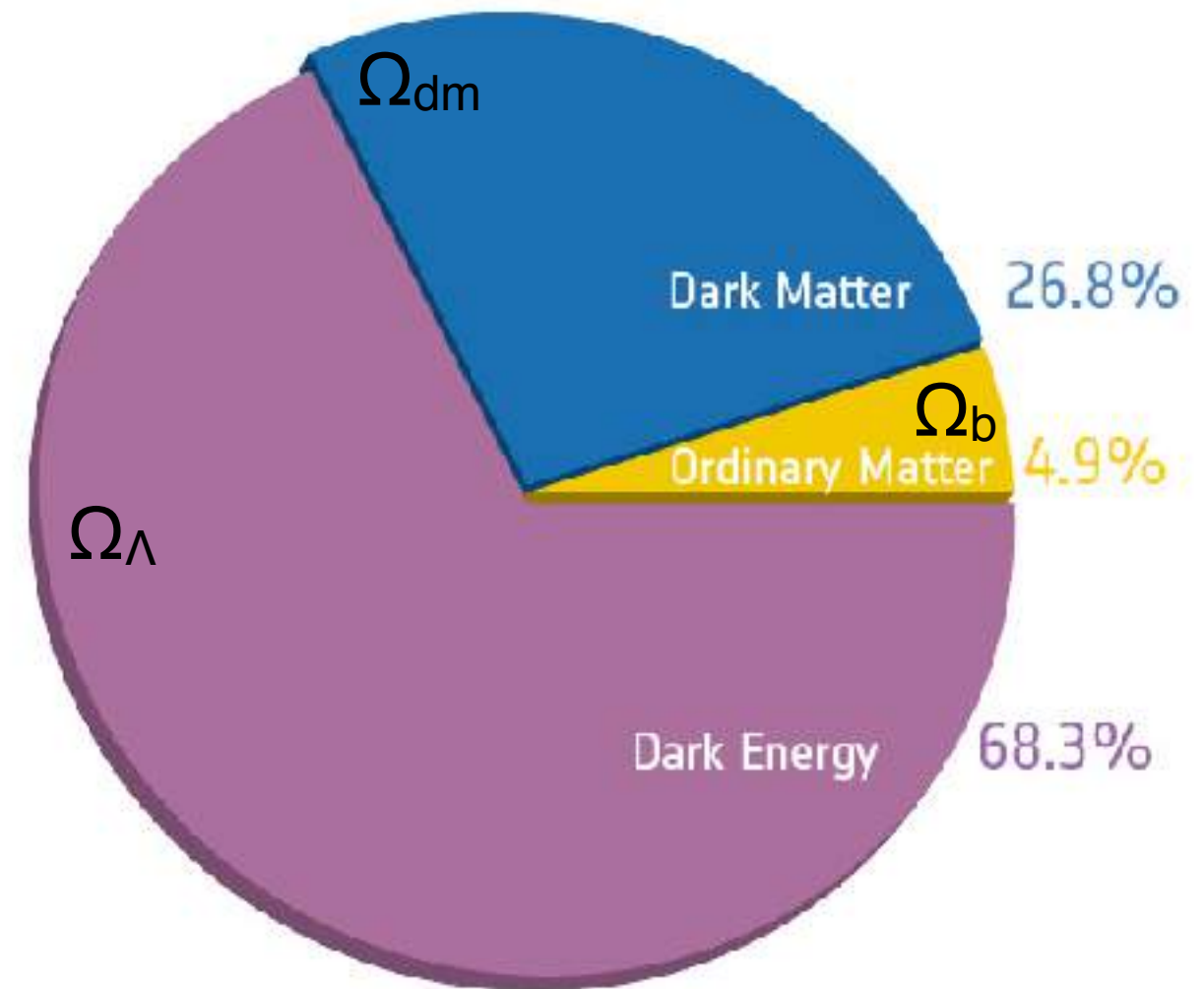
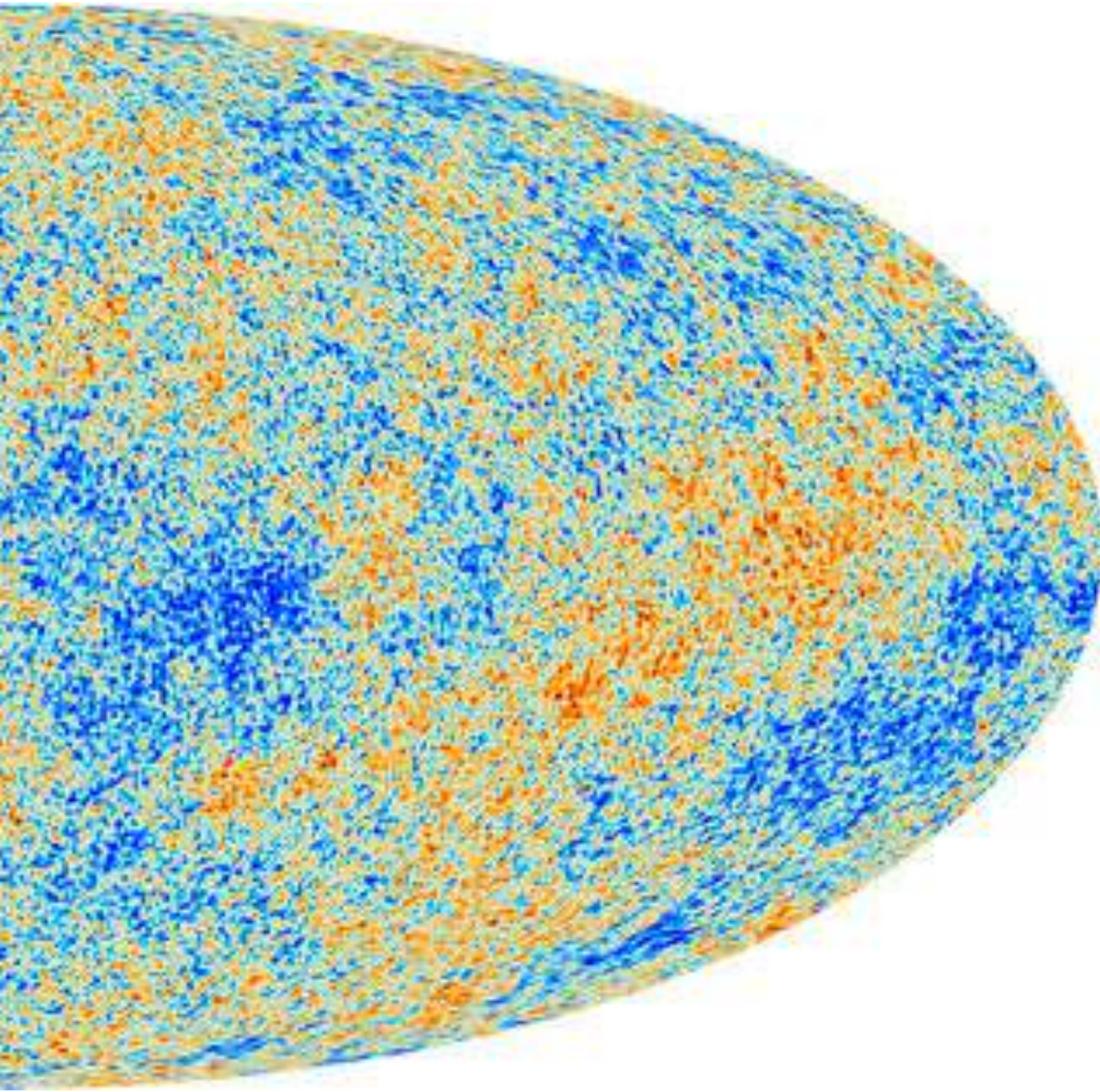
disk $R_{s,\star} \sim \text{few kpc}$

- viral radius of halo

$R_{200c} \sim 200 \text{ kpc}$

because baryons can radiate away their energy and condense but dark matter cannot, so is supported in larger structures by internal kinetic energy

The standard Λ Cold Dark Matter cosmology

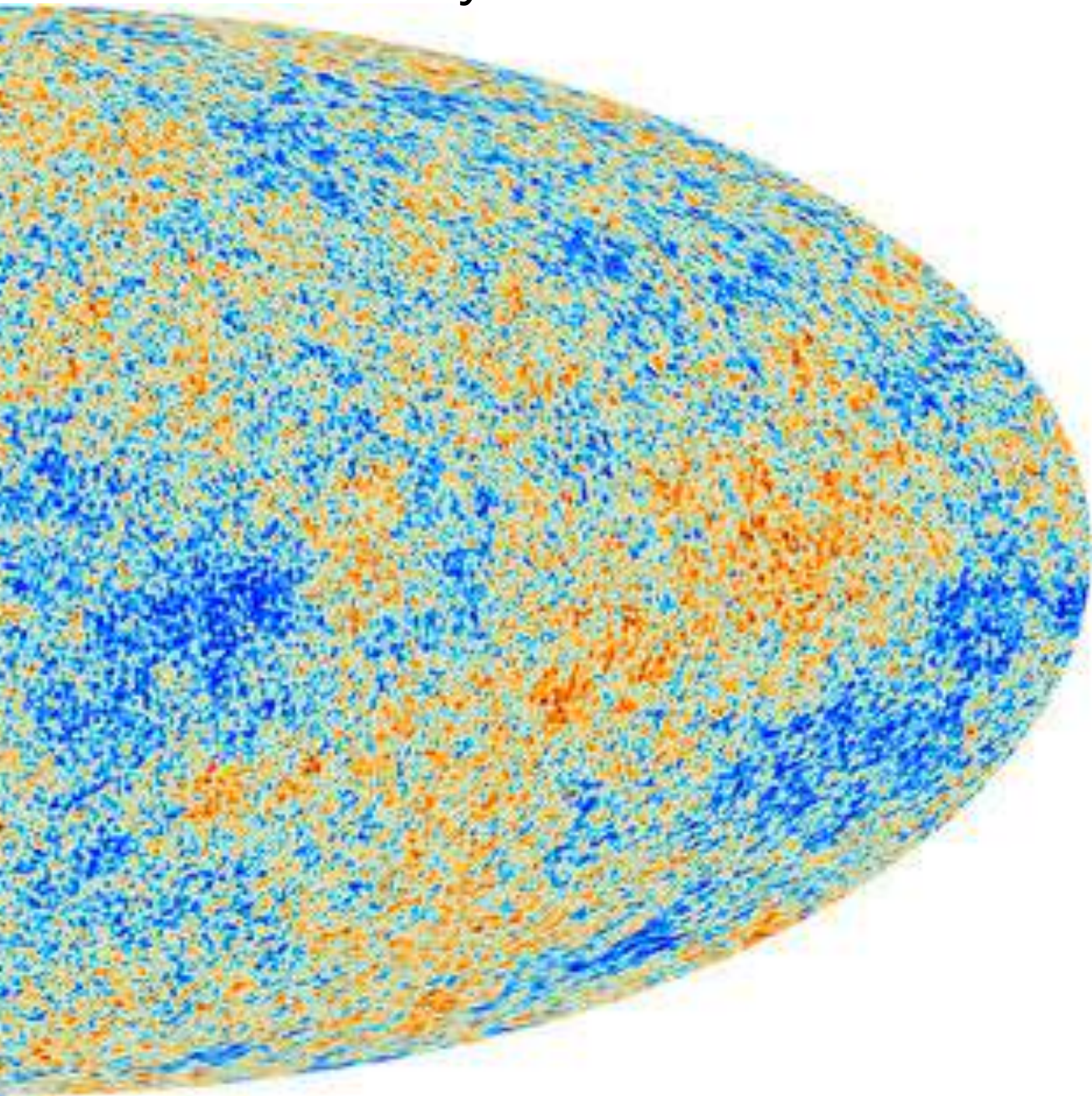


Combined with other astronomical measurements, the cosmic microwave background tells us:

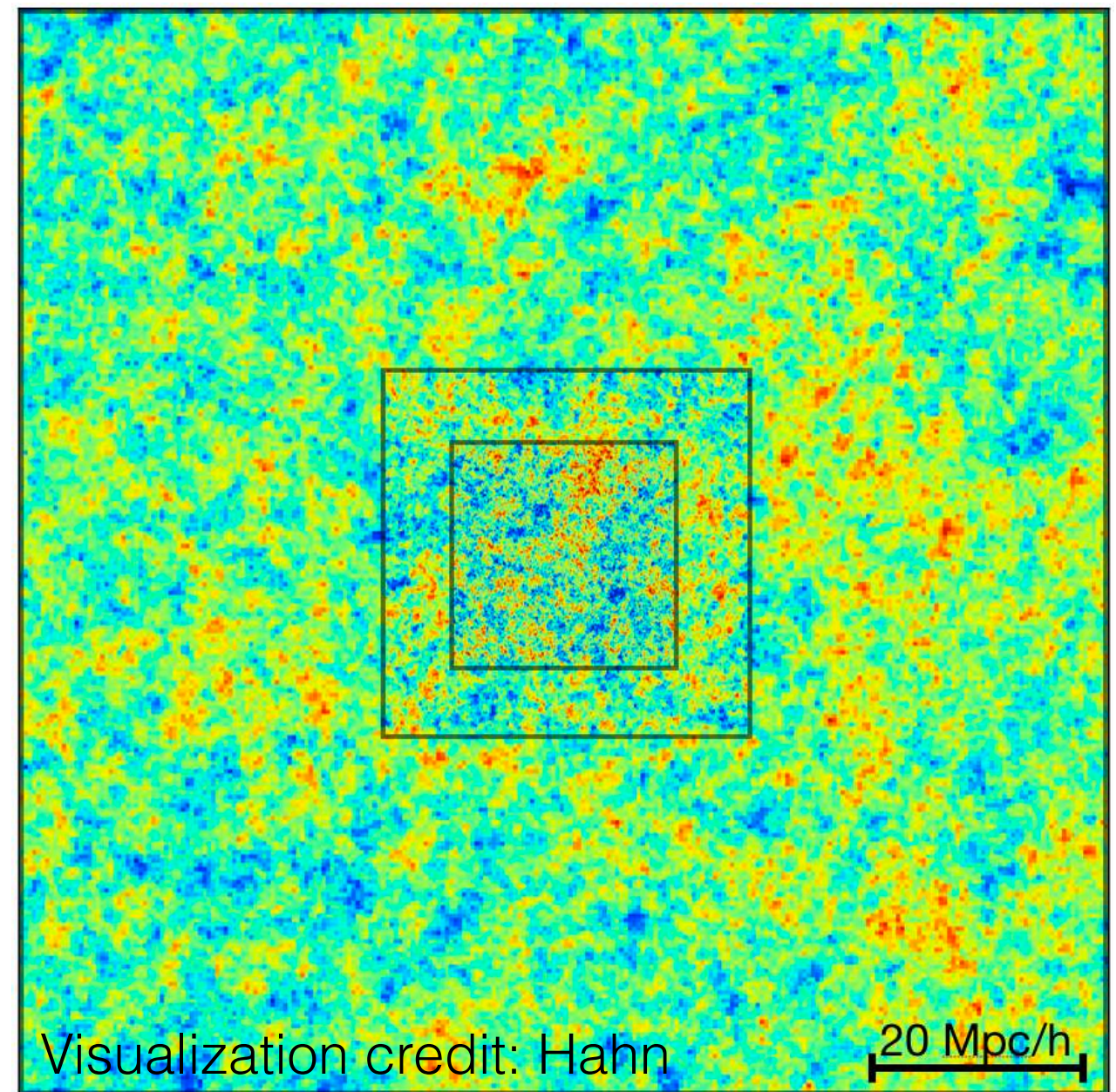
- ▶ spectrum of initial density fluctuations
- ▶ what the Universe is made out of
- ▶ how old it is and how it has expanded in time

Cosmological initial conditions

Microwave sky



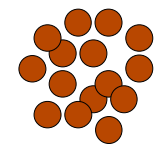
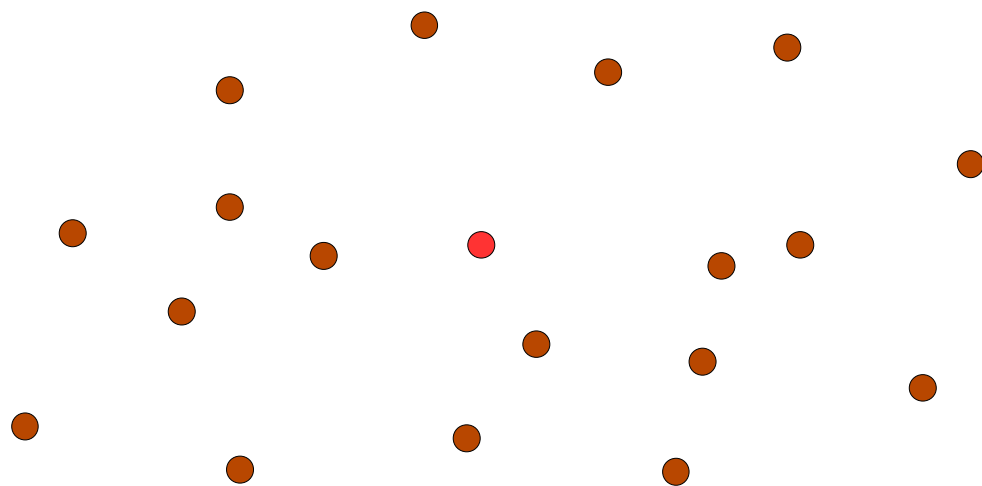
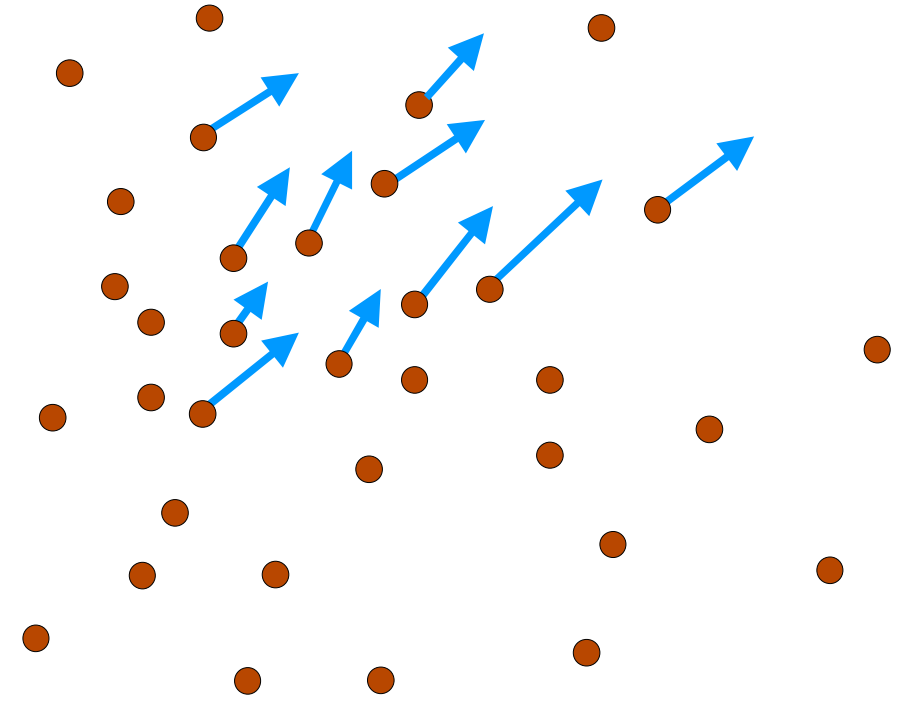
Simulation ICs



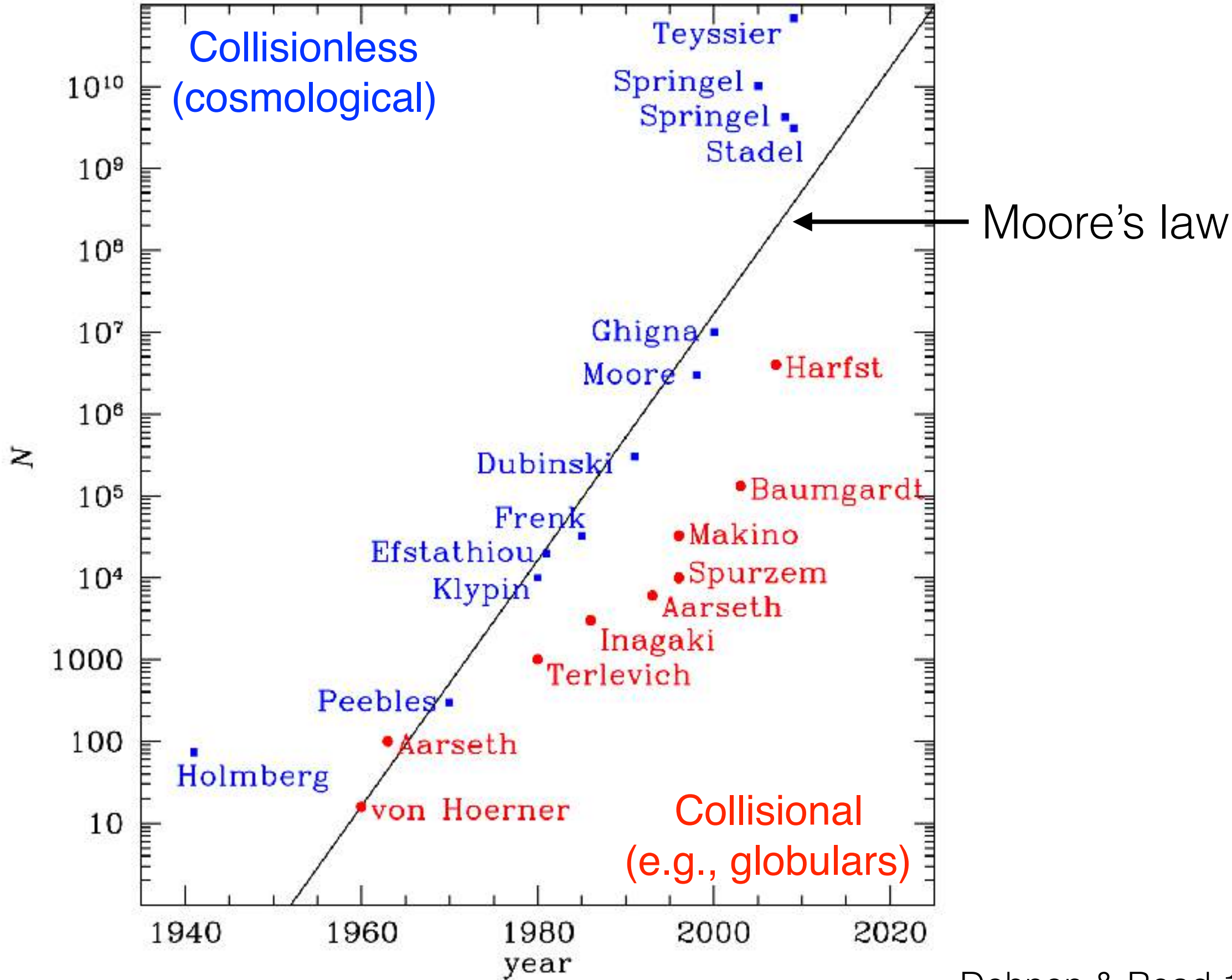
Gaussian random field filtered with "transfer function" to model early Universe physics (photon-baryon interactions)

N -body simulations

- Discretize mass with N particles
 - ▶ in cosmology, usually tree or particle-mesh methods to solve Poisson's equation
- Naturally adaptive in cosmology



History of N-body simulations



Structure formation in Λ cold dark matter

cosmological N -body simulation showing dark matter evolution



baryons cool at center of dark matter halos, fragment into stars

Dark matter in Millennium simulation (z=0 fly-through)

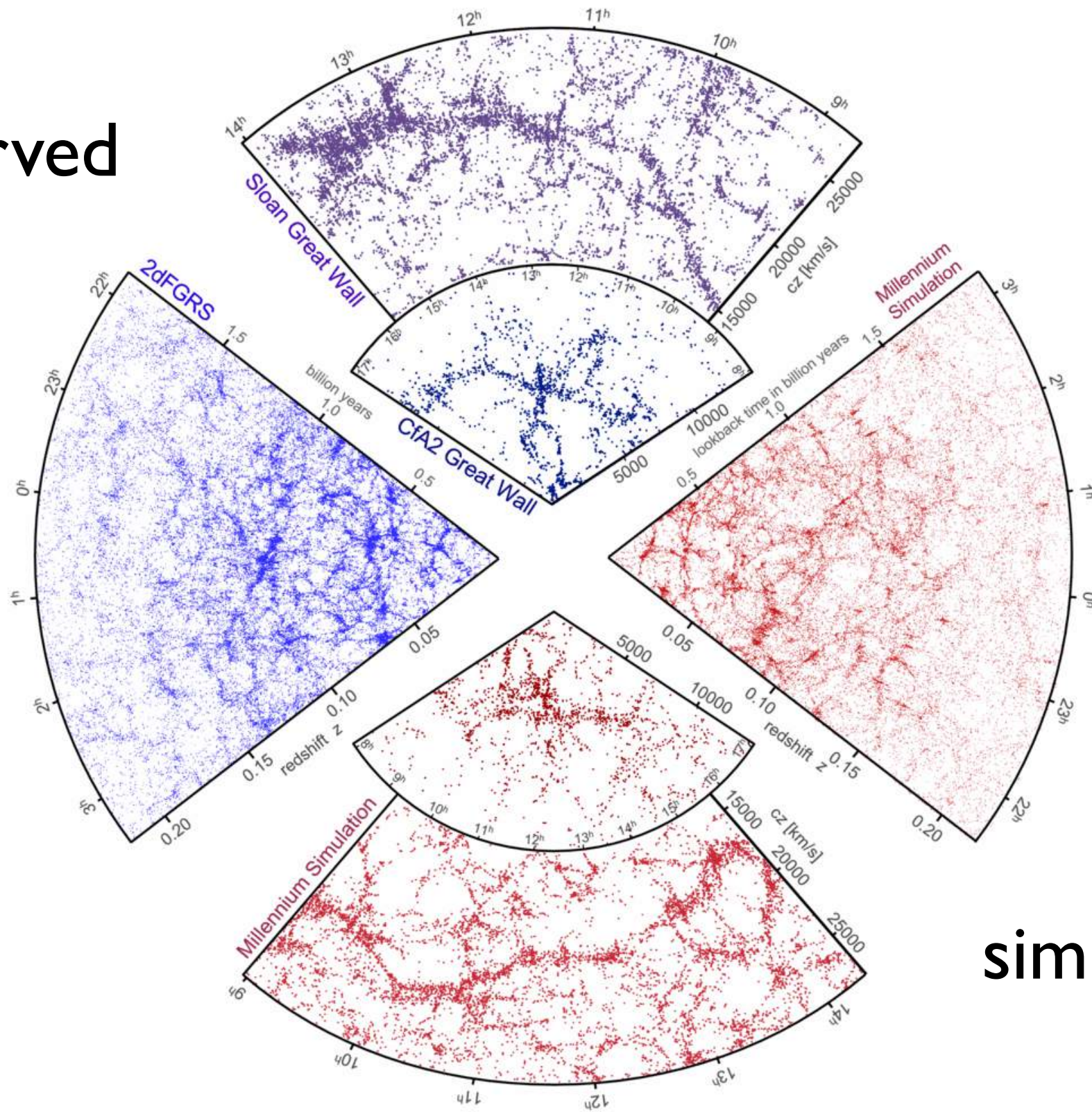


10^{10} particles, 700 Mpc

Springel+05

Statistically, the model galaxy distribution agrees well with observations

observed



simulated

Dark matter halo mass function

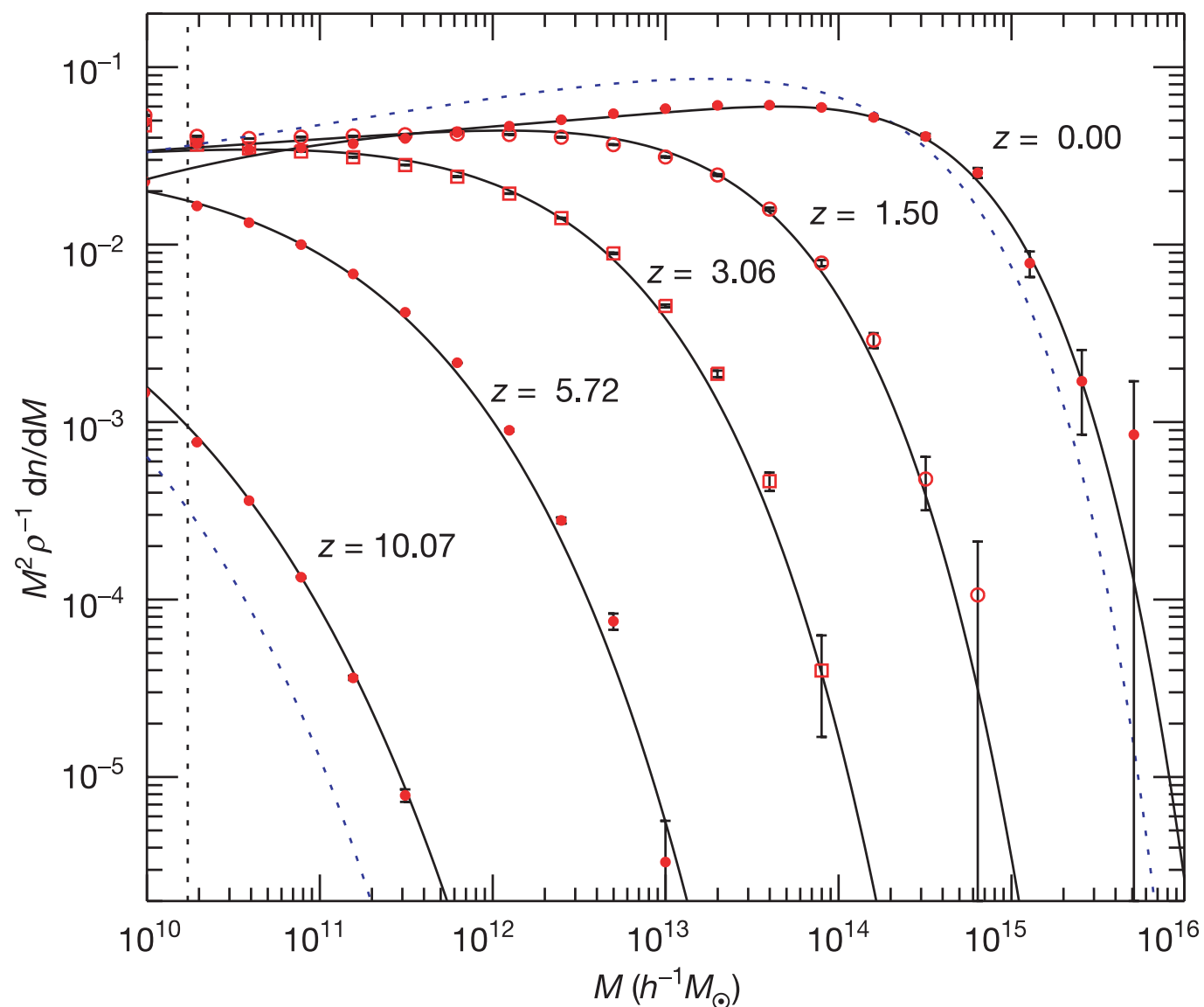


Figure 2 | Differential halo number density as a function of mass and epoch. The function $n(M, z)$ gives the co-moving number density of haloes less massive than M . We plot it as the halo multiplicity function $M^2 \rho^{-1} dn/dM$ (symbols with $1-\sigma$ error bars), where ρ is the mean density of the Universe. Groups of particles were found using a friends-of-friends algorithm⁶ with linking length equal to 0.2 of the mean particle separation. The fraction of mass bound to haloes of more than 20 particles (vertical dotted line) grows from 6.42×10^{-4} at $z = 10.07$ to 0.496 at $z = 0$. Solid lines are predictions from an analytic fitting function proposed in previous work¹¹, and the dashed blue lines give the Press-Schechter model¹⁴ at $z = 10.07$ and $z = 0$.

halos per volume per mass interval

dimensionless when expressed in terms of ‘multiplicity function’

massive halos $> M_*$

exponentially suppressed (e.g., galaxy clusters today)

MW halo $\approx 10^{12} M_{\text{sun}}$

Press-Schechter is analytic derivation; better fits given by Seth-Tormen function

(Nearly) universal dark matter halo profile

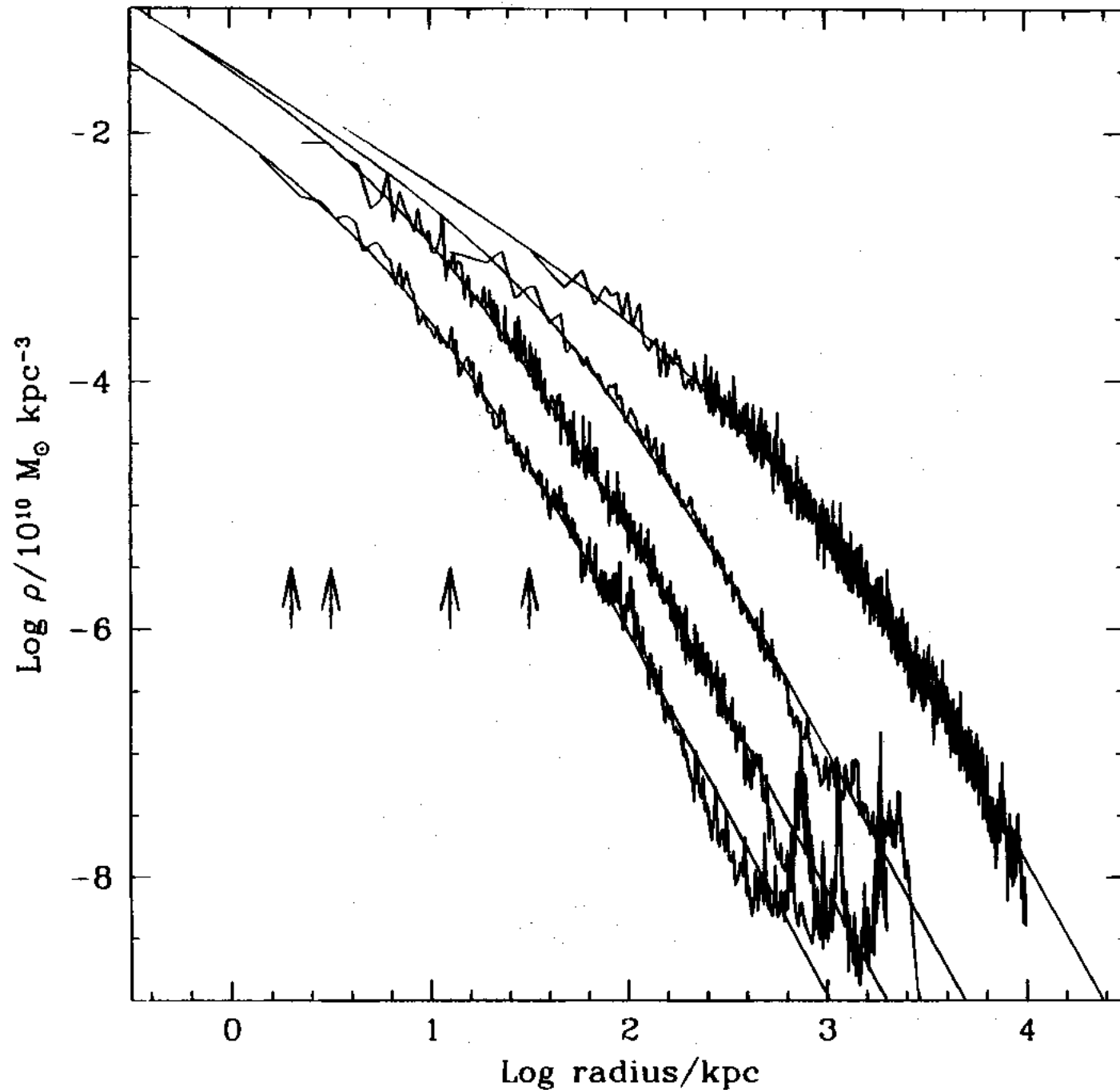


FIG. 3.—Density profiles of **four halos spanning 4 orders of magnitude** in mass. The arrows indicate the gravitational softening, h_g , of each simulation. Also shown are fits from eq. (3). The fits are good over two decades in radius, approximately from h_g out to the virial radius of each system.

NFW profile

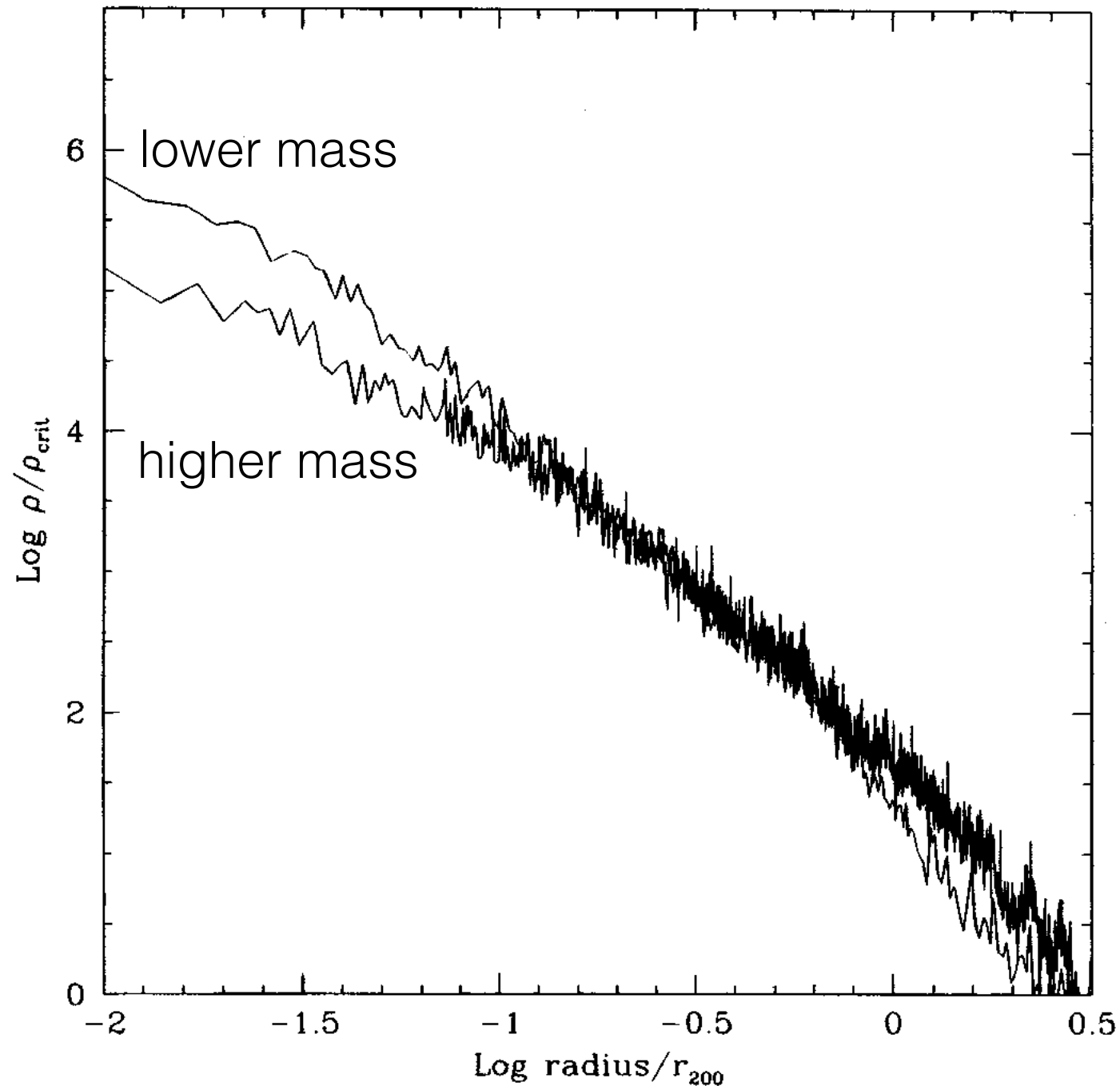
$$\frac{\rho(r)}{\rho_{\text{crit}}} = \frac{\delta_c}{(r/r_s)(1 + r/r_s)^2}$$

$$\delta_c = \frac{200}{3} \frac{c^3}{[\ln(1 + c) - c/(1 + c)]}$$

$$r_s = r_{200}/c$$

fits halos of all masses in N -body sims

Halo concentration



Lower-mass halos are more concentrated (form earlier, when Universe was denser)

FIG. 4.— Scaled density profiles of the most and least massive halos shown in Fig. 3. The large halo is less centrally concentrated than the less massive system.

Concentration correlates with halo mass

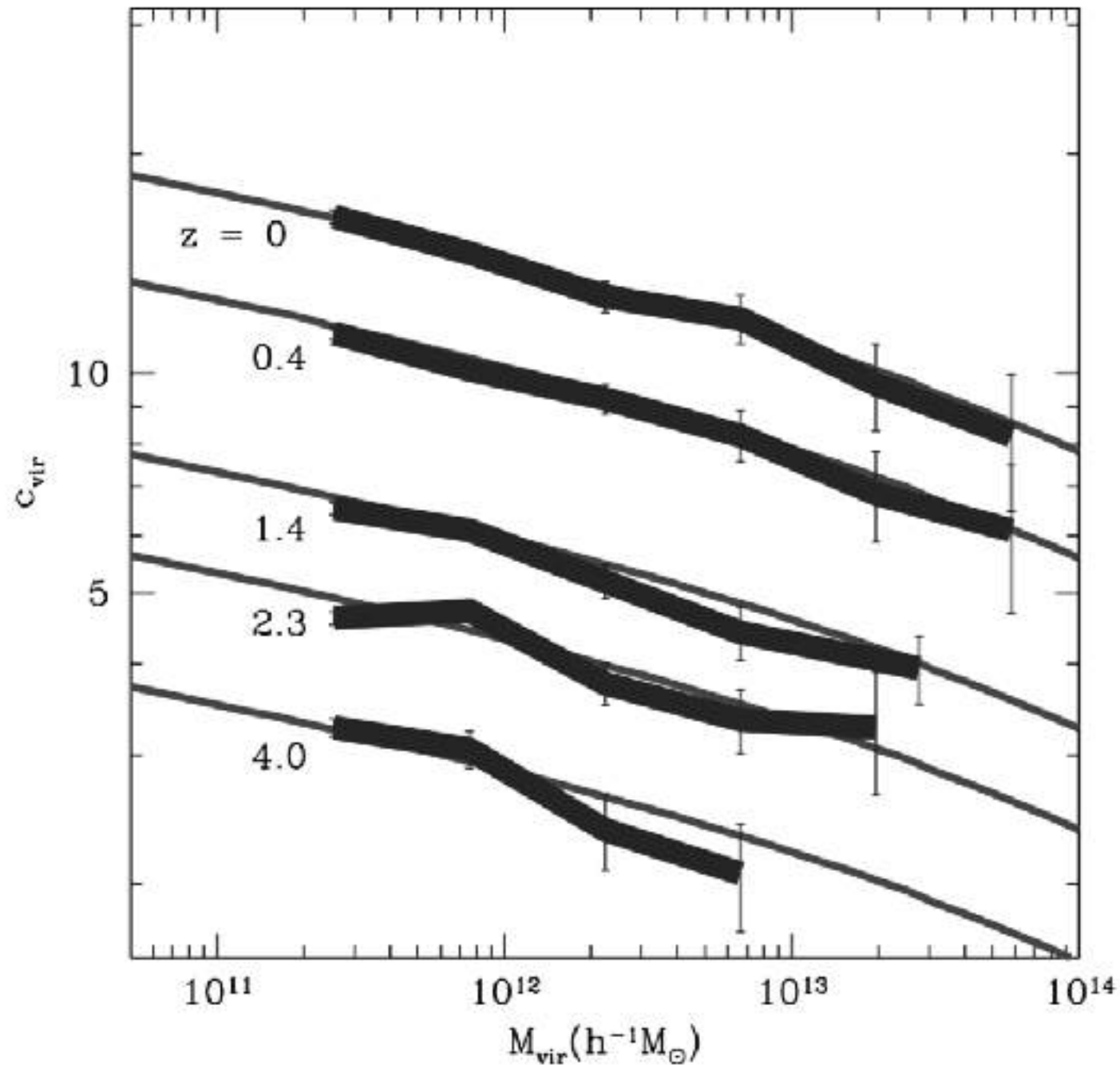


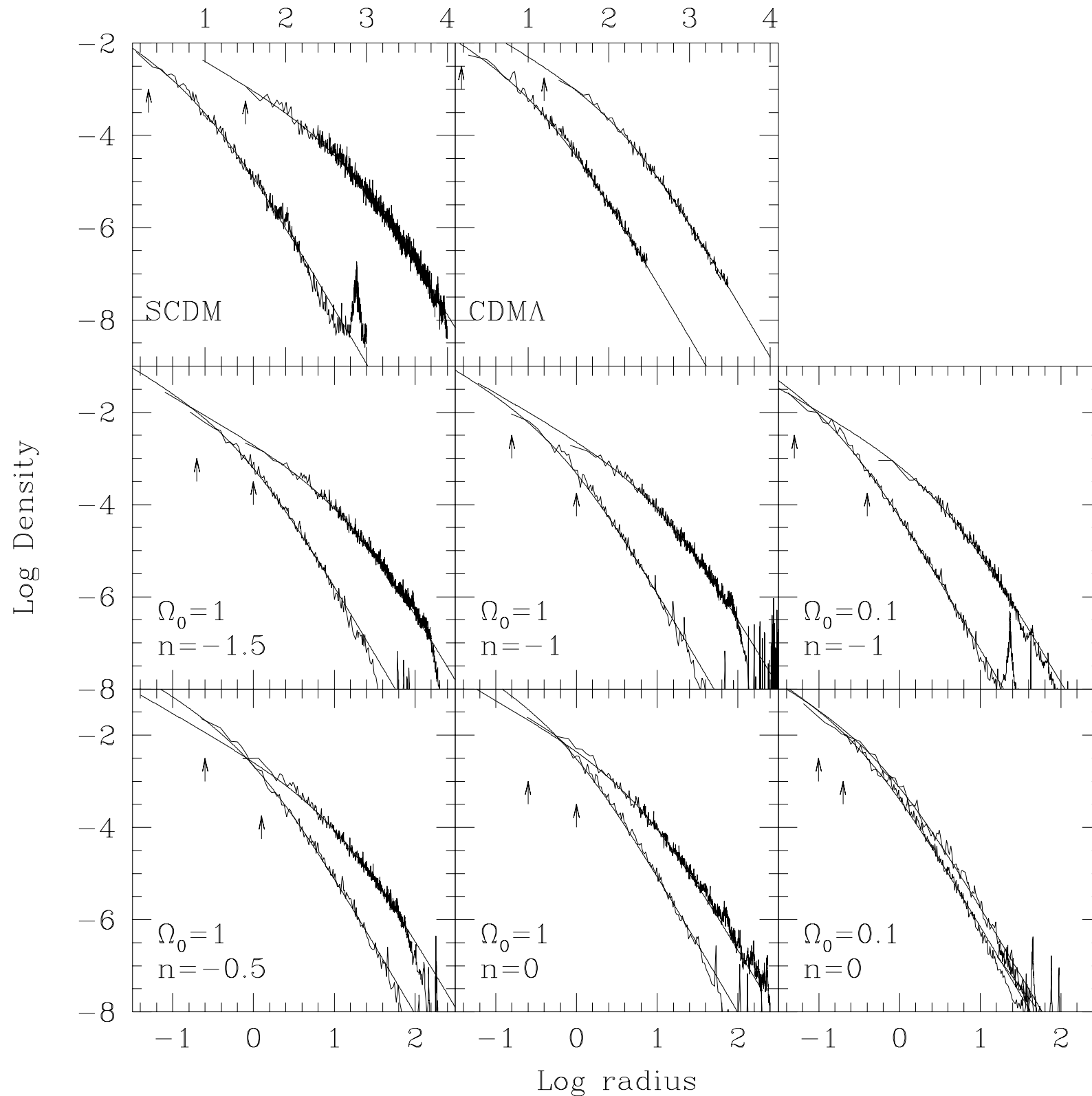
Figure 10. Median c_{vir} values as a function of M_{vir} for distinct haloes at various redshifts. The error bars are the Poisson errors due to the finite number of haloes in each mass bin. The thin solid lines show our toy model predictions.

Dark matter halo profiles form an (approximately) two-parameter family (M_{200} and z)

[Historical note: original NFW paper focused on $z=0$ so said ‘one-parameter’ family]

$$c \approx 15 \left(\frac{M_{200}}{10^{12} M_{\odot}} \right)^{-0.2} (1+z)^{-1}$$

NFW profile is a generic outcome of CDM models

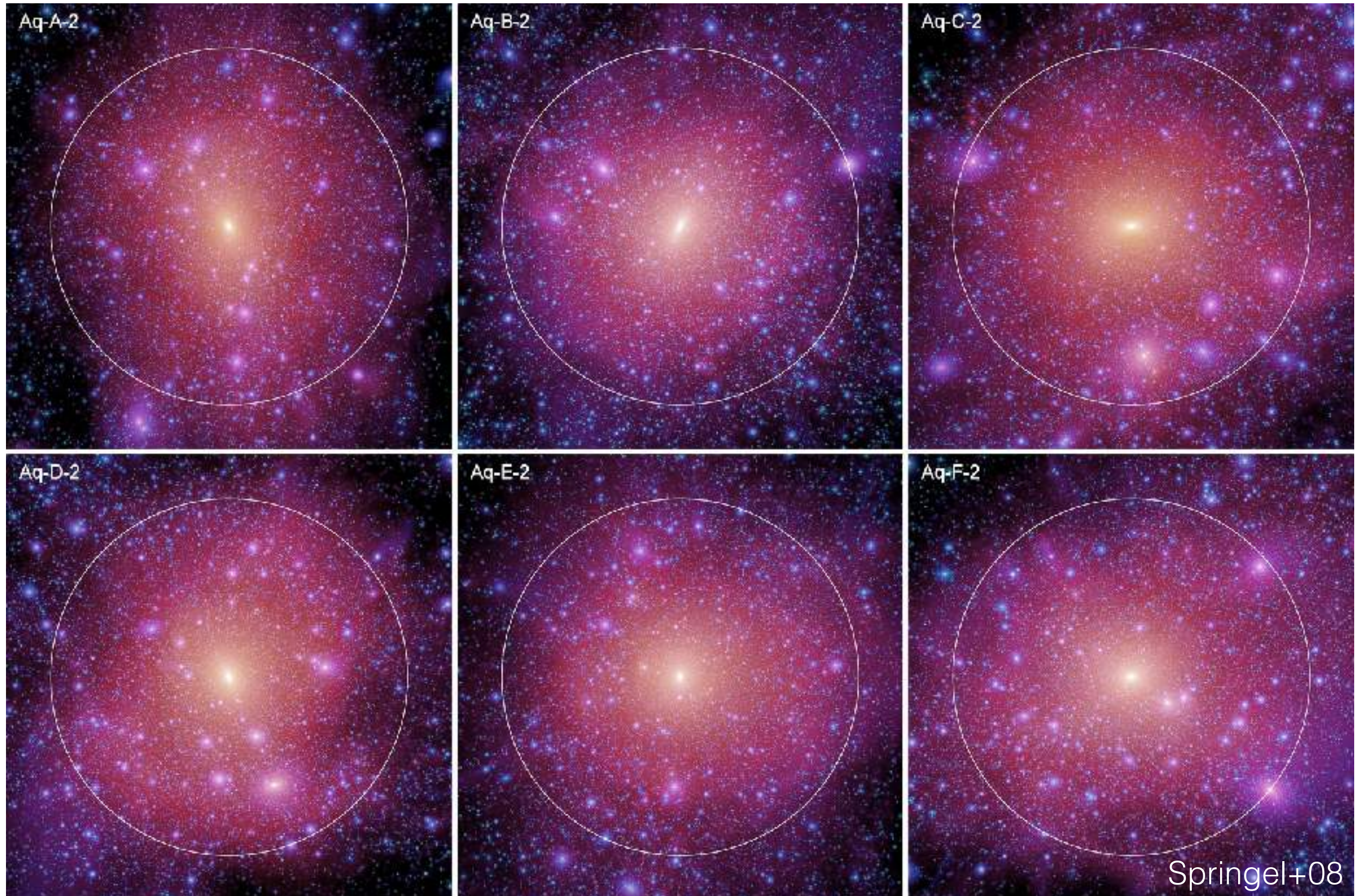


In CDM simulations,
NFW emerges
independent of
cosmological
parameters (e.g.,
 $\Omega_m \equiv \Omega_0$) and power
spectrum of initial
conditions (spectral
index n)

still not fully understood

FIG. 2.—Density profiles of one of the most massive halos and one of the least massive halos in each series. In each panel, the low-mass system is represented by the leftmost curve. In the SCDM and CDM models, radii are given in kiloparsecs (*scale at top*), and densities are in units of $10^{10} M_\odot \text{kpc}^{-3}$. In all other panels, the units are arbitrary. The density parameter, Ω_0 , and the value of the spectral index, n , are given in each panel. The solid lines are fits to the density profiles using eq. (1). The arrows indicate the value of the gravitational softening. The virial radius of each system is in all cases 2 orders of magnitude larger than the gravitational softening.

Aquarius zoom-in simulations (dark matter only)



6 $M_h \sim 10^{12} M_{\text{sun}}$ halos, ultra-high res. (up to 10^9 particles within R_{vir})

Einasto profile $\frac{d \log \rho}{d \log r} = -2 \left(\frac{r}{r_{-2}} \right)^\alpha$ is better fit at small radius

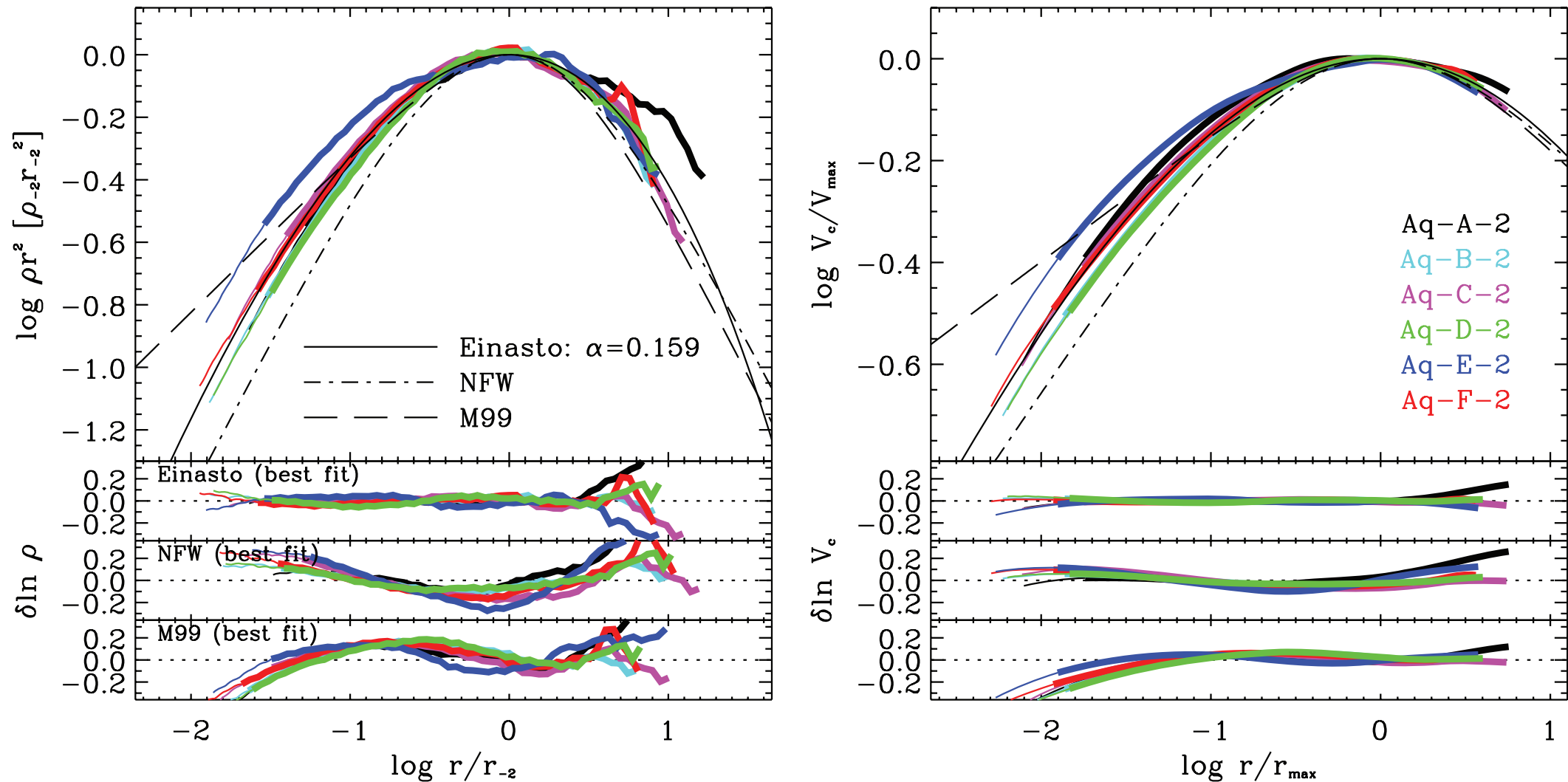
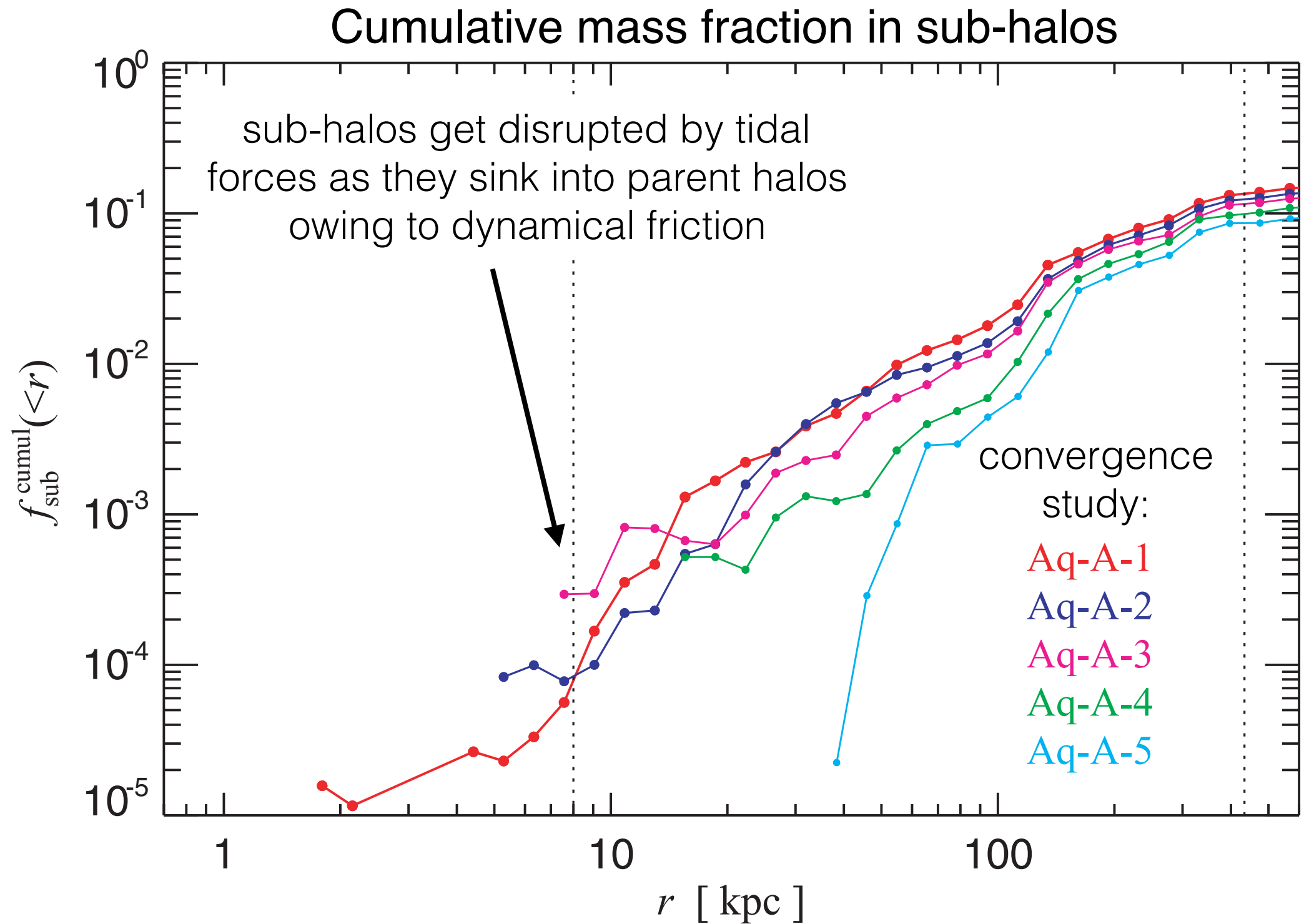


Figure 3. Left-hand panel: spherically averaged density profiles of all level-2 Aquarius haloes. Density estimates have been multiplied by r^2 in order to emphasize details in the comparison. Radii have been scaled to r_{-2} , the radius where the logarithmic slope has the ‘isothermal’ value, -2 . Thick lines show the profiles from $r_{\text{conv}}^{(7)}$ outwards; thin lines extend inwards to $r_{\text{conv}}^{(1)}$. For comparison, we also show the NFW and M99 profiles, which are fixed in these scaled units. This scaling makes clear that the inner profiles curve inwards more gradually than NFW, and are substantially shallower than predicted by M99. The bottom panels show residuals from the *best fits* (i.e. with the radial scaling free) to the profiles using various fitting formulae (Section 3.2). Note that the Einasto formula fits all profiles well, especially in the inner regions. The shape parameter, α , varies significantly from halo to halo, indicating that the profiles are not strictly self-similar: no simple physical rescaling can match one halo on to another. The NFW formula is also able to reproduce the inner profiles quite well, although the slight mismatch in profile shapes leads to deviations that increase inwards and are maximal at the innermost resolved point. The steeply cusped Moore profile gives the poorest fits. Right-hand panel: same as the left, but for the circular velocity profiles, scaled to match the peak of each profile. This cumulative measure removes the bumps and wiggles induced by substructures and confirms the lack of self-similarity apparent in the left-hand panel.

Note: Einasto is Sérsic with I replaced by ρ and R (projected) replaced by r (3D)

Dark matter substructure



≈ 10% halo mass in sub-halos

Extra slides

Quantitative relationship between galaxy and halo sizes

Can use *abundance matching*
(most massive galaxies in most
massive halos) to connect galaxy
to halo properties

At $z=0$, $r_{1/2} \approx 0.015 R_{200}$

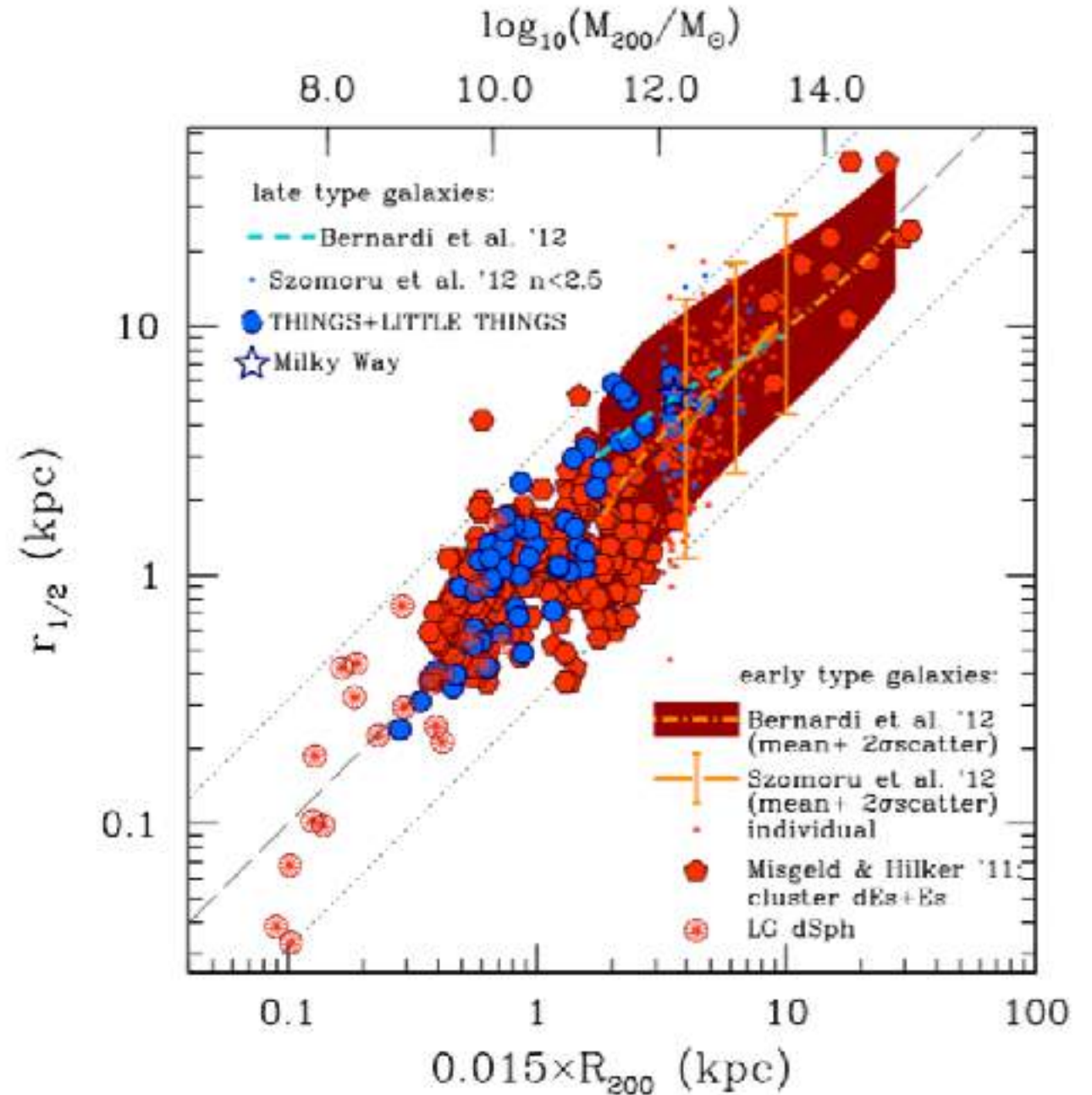


Figure 1. Relation between the half-mass radius of stellar distribution in galaxies of different stellar masses (spanning more than eight orders of magnitude in stellar mass) and morphological types and inferred virial radius of their parent halos, R_{200} , defined as the radius enclosing overdensity of $200\rho_{\text{cr}}$, and estimated as described in Section 2. The red and orange symbols and lines show early-type galaxies, while blue and cyan symbols and line show late-type galaxies, as indicated in the figure legend (see Sections 3 and 4.1 for details). The gray dashed line shows linear relation $r_{1/2} = 0.015 R_{200}$ and dotted lines are linear relations offset by 0.5 dex, which approximately corresponds to the 2σ scatter $2\sigma_{\ln\lambda} \approx 1.1$ expected for dark matter halos.